Anal. Chem. **2001,** *73,* 2501−2508

Optical Multibead Arrays for Simple and Complex Odor Discrimination

Keith J. Albert and David R. Walt*

The Max Tishler Laboratory for Organic Chemistry, Department of Chemistry, Tufts University, Medford, Massachusetts 02155

Daljeet S. Gill and Tim C. Pearce*

Department of Engineering, University of Leicester, Leicester LE1 7RH, United Kingdom

A fiber optic bead-based sensor array platform has been employed to discriminate between six different odors and air carrier gas. Six different bead sensor types, with over 250 replicates of each, were monitored before, during, and after odor exposure to produce time-dependent fluorescence response patterns that were unique for each sensor−analyte combination. A total of 2683 sensors were analyzed with respect to changes in their fluorescence, and signals from identical sensor beads were averaged to improve signal-to-noise ratios. Analyte classification rates of 100% were achieved for three complex (coffee bean) odors and three pure (simple) odors (toluene, acetone, 1,3-dinitrotoluene) measured at their highest relative concentrations. When lower odor concentrations were employed, the system exhibited better than 85% classification rates for analyte discrimination. Sensor response repeatability to these odor stimuli has also been quantified statistically, which is vital in defining the detection limit of the overall system. These results demonstrate, for the first time, the utility of our bead array technology for discriminating between different odor types at various dilution levels.

Over the last two decades, there has been an increase in the development of odor detection systems that utilize cross-reactive sensor arrays in conjunction with pattern recognition techniques to interpret array response patterns.[1−10] These sensor array systems have been referred to, variously, as artificial, or electronic noses and are playing an increasing role as screening tools to complement existing analytical techniques. The development of odor detection systems is progressively moving toward systems that mimic, on some or many levels, the vertebrate's olfactory system. It is believed that the olfactory receptor neurons are cross-sensitive and create neuronal response patterns[11] that are used as a basis for identifying aromas as pungent, putrid, flowery, etc., even though the components within the aroma are never quantified directly or individually identified. In the same way that mixtures of odor molecules create unique response patterns in the olfactory bulb, which the brain subsequently interprets as a particular odor quality, artificial nose systems rely on response patterns of physical or chemical molecular characteristics that can be attributed to an odor observation without quantifying every component. In such systems, sensor−analyte response patterns are used to train statistical classifiers for subsequent odor interpretation, discrimination, and/or quantification.[7−10] This technology can be applied in situations where it is not necessary to know an odor's composition in detail[12] but is instead used to detect changes in odor characteristics, even in a complex (sometimes interfering) background, i.e., such as monitoring the presence/absence of low-level explosives-like nitroaromatic compounds (NAC).[13−16] Classification of complex odors or odor environments is a much more difficult task because of overall odor complexity; e.g., coffee odors usually contain hundreds of odorous compounds.[17] Despite the complex nature of some odors, sensor array systems have been able to discriminate between different types of coffee[18−21] and one such study determined the minimum number of sensors and transducers needed to obtain complete

* Corresponding authors. For sensor work, D.R.W.: (fax) 617.627.3443; (e-mail) david.walt@tufts.edu. For computational work, T.C.P.: (phone) +44-(0)116.223.1290; (fax) +44(0)116.252.2619; (e-mail) t.c.pearce@leicester.ac.uk.

(1) Persaud, K. C.; Dodd, G. H. *Nature* **1982**, *299*, 352−355.
(2) Carey, W. P.; Beebe, K. R.; Kowalski, B. R. *Anal. Chem.* **1987**, *57*, 1529−1534.
(3) Gardner, J. W.; Bartlett, P. N. *Electronic Noses: Principles and Applications*; Oxford University Press: Oxford, U.K., 1999.
(4) Lonergan, M. C.; Severin, E. J.; Doleman, B. J.; Beaber, S. A.; Grubbs, R. H.; Lewis, N. S. *Chem. Mater.* **1996**, *8*, 2298−2312.
(5) Stetter, J. R.; Jurs, P. C.; Rose, S. L. *Anal. Chem.* **1986**, *58*, 860−866.
(6) Albert, K. J.; Lewis, N. S.; Schauer, C. L.; Sotzing, G. A.; Stitzel, S. E.; Vaid, T. P.; Walt, D. R. *Chem. Rev.* **2000**, *100*, 2595−2626.
(7) Jurs, P. C.; Bakken, G. A.; McClelland, H. E. *Chem. Rev.* **2000**, *100*, 2649−2678.
(8) Gardner, J. W. *Sens. Actuators B* **1992**, *4*, 109−115.
(9) Shaffer, R. E.; Rose-Pehrsson, S. L.; McGill, R. A. *Anal. Chim. Acta* **1999**, *384*, 305−317.
(10) Hines, E. L.; Llobet, E.; Gardner, J. W. *IEE Proc.-Circuits Devices Syst.* **1999**, *146*, 297−310.
(11) Sicard, G.; Holley, A. *Brain Res.* **1984**, *292*, 283−296.
(12) Rouhi, M. *Chem. Eng. News* **1999**, *75* (Mar 29), 58.
(13) Albert, K. J.; Walt, D. R. *Anal. Chem.* **2000**, *72*, 1947−1955.
(14) Bakken, G. A.; Kauffman, G. W.; Jurs, P. C.; Albert, K. J.; Stitzel, S. E., *Sens. Actuators B*, in press.
(15) Albert, K. J.; Myrick, M. L.; Brown, S. B.; James, D. L.; Milanovich, F.; Walt, D. R., *Environ. Sci. Technol.*, in press.
(16) Stitzel, S. E.; Cowen, L.; Albert, K. J.; Walt, D. R., manuscript submitted.
(17) Clarke, R. J., Macrae, R., Eds. *Coffee*; *Chemistry*; Elsevier Applied Science Publishers: New York, 1985; Vol. 1.
(18) Legin, A.; Rudnitskaya, A.; Vlasov, Y.; Di Natale, C.; Davide, F.; D'Amico, A. *Sens. Actuators B* **1997**, *44*, 291−296.

10.1021/ac001137a CCC: $20.00
Published on Web 05/04/2001

Table 1. Microsensor Materials Employed

sensor name	size (μm)	microsphere material[a]	surface modification[b]	pore size (Å)	no. of sensors analyzed
A	5	Chirex	3012[c]	not known	814
B	5	Spherex	aniline	100	286
C	3	Phenosphere	cyano (CN)	80	301
D	3	Phenosphere	hydroxy (OH)	80	692
E	5	Develosil	hydroxyl (OH)	60	294
F	5	Phenosphere	cyano (CN)	80	296

[a] Materials are named according to the distributor (Phenomenex, Torrance, CA). [b] Materials were either purchased or modified with particular surface functionalities. All sensors were stained with Nile Red dye and stored dry, except sensor type **C**, which was stored in 0.01% Tween/DI water (see Experimental Section). [c] (*R*)-Phenylglycine and 3,5-dinitroaniline urea linkage.

discrimination between three coffee brands and three mixtures of the brands.[22]

Here, we report on our use of a combined optical imaging and sensor array system to discriminate between six odor conditions, including three different coffee types, and air (control) carrier gas. The system is based on previously developed cross-reactive array technology[23,24] and incorporates optical imaging fibers, which are high-density arrays of micrometer-scale optical fibers,[25] as our sensor platform. The imaging fiber's distal face is chemically etched to create an array of "optically wired" addressable microwells on the fiber's tip,[26] into which complementary-sized microsphere sensors are incorporated.[27] The microspheres have the solvatochromic dye Nile Red[28−30] adsorbed on their surface, which undergo intensity and/or wavelength shifts upon microenvironmental polarity changes. During odor exposure, each sensor type produces a unique temporal fluorescence response profile depending on sensor−analyte interactions, i.e., odor polarity and diffusion. These sensor materials have been well documented for optically based odor detection techniques.[13−16,31] This sensor array platform has recently been shown to detect low-level NACs in higher background concentration levels of volatile organic compounds (VOCs) with 100% accuracy.[14] We now employ an array with more sensor types to show, for the first time, that high-density arrays of cross-reactive bead sensors can detect and discriminate between simple and complex odors at various analyte dilutions. We also report on a new method for automatically extracting sensor−analyte response profiles and for compensating for small shifts, e.g., array movement, within the source image. This new image analysis technique may eventually facilitate real-time monitoring, which is of paramount importance for many chemical detection problems (security, food quality, medicinal diagnostics, mine detection, etc.). Sensor response repeatability from run to run to the above odor stimuli has also been quantified statistically, which is important since it limits the detection of the microsensor technology in a practical chemical sensing application.[32]

EXPERIMENTAL SECTION

Materials. Acetone, ethanol, and toluene were purchased from Fisher (Pittsburgh, PA). Nile Red dye, *N*-[3-(trimethoxysilyl)-propyl]aniline, and 1,3-dinitrobenzene (1,3-DNB) were purchased from Aldrich (Milwaukee, WI) and used as received. Hazelnut-flavored, French roast, and Columbian coffee beans (Jim's Organic Coffee) were used as purchased. The carrier gas used in the experiments is ultra zero grade air from Northeast Gas, Inc. (Salem, NH). A 1010 Precision gas diluter (tedlar bag gas dilution system) and analyte bags were purchased from Custom Sensor Solutions, Inc. (Naperville, IL). Tween 20 was obtained from J. T. Baker Chemical Co. (Phillipsburg, NJ). The excitation filters employed were purchased from Chroma Technology Corp. (Brattleboro, VT). The pre-etched, optical imaging fibers (with 3.19- and 5.5-μm core diameters) were purchased from Illumina, Inc. (San Diego, CA). Six different types of porous silica microsphere packing material were removed from HPLC columns (Phenomenex, Torrance, CA) and employed as substrates to which the fluorescent dye is physisorbed (Table 1).

Bead Sensor Fabrication. All sensors, except B, were prepared as described previously.[13] Briefly, the porous silica microspheres were rinsed thoroughly with ethanol and allowed to dry in room air overnight. Each microsphere type was individually stained with a solution of 0.5 mg/mL Nile Red in toluene by placing ~50 mg of microsphere material on a vacuum filtration system, rinsing with toluene, and then passing the Nile Red solution over the beads. Nile Red is readily sorbed to the surface of the modified porous silica microspheres, and excess dye was removed by subsequent rinsing steps with toluene and deionized water. See Supporting Information for sensor B fabrication details. All beads were stored dry, except C. One day before data collection, approximately 30 mg of C was added to a 1-mL solution of 0.01% Tween 20 in deionized water.

Array Fabrication. Six pre-etched, imaging fibers were employed and all sensors except C were distributed into the wells

(19) Singh, S.; Hines, E. L.; Gardner, J. W. *Sens. Actuators B* **1996**, *30*, 185−190.
(20) Gardner, J. W.; Shurmer, H. V.; Tan, T. T. *Sens. Actuators B* **1992**, *6*, 71−75.
(21) Llobet, E.; Hines, E. L.; Gardner, J. W.; Bartlett, P. N.; Mottram, T. T. *Sens. Actuators B* **1999**, *61*, 183−190.
(22) Ulmer, H.; Mitrivics, J.; Noetzel, G.; Weimar, U.; Gopel, W. *Sens. Actuators B* **1997**, *43*, 24−33.
(23) Dickinson, T. A.; White, J.; Kauer, J. S.; Walt, D. R. *Nature* **1996**, *382*, 697−700.
(24) White, J.; Kauer, J. S.; Dickinson, T. A.; Walt, D. R. *Anal. Chem.* **1996**, *68*, 2191−2202.
(25) Pantano, P.; Walt, D. R. *Anal. Chem.* **1995**, *67*, A481−A487.
(26) Pantano, P.; Walt, D. R. *Chem. Mater.* **1996**, *8*, 2832−2835.
(27) Michael, K. L.; Taylor, L. C.; Shultz, S. L.; Walt, D. R. *Anal. Chem.* **1998**, *70*, 1242−1248.
(28) Vauthey, E. *Chem. Phys. Lett.* **1993**, *216*, 530−536.
(29) Meinershagen, J. L.; Bein, T. *J. Am. Chem. Soc.* **1999**, *121*, 448−449.
(30) Deye, J. F.; Berger, T. A. *Anal. Chem.* **1990**, *62*, 615−622.
(31) Dickinson, T. A.; Michael, K. M.; Kauer, J. S.; Walt, D. R. *Anal. Chem.* **1999**, *71*, 2192−2198.
(32) Pearce, T. C.; Verschure, P. F. M. J. V.; White, J.; Kauer, J. S. *Neurocomputing*, in press.

by a dry deposition process as described previously.[13] Sensor C was deposited onto the fiber's etched face by removing 2 μL of the bead/Tween 20 solution and placing onto the etched face. As the solution dried, the beads assembled spontaneously into the wells (one sensor per well). Excess beads were removed with a sharp burst of air from a dry air gun (2-s air pulse). The six fibers were separated into two groups of three fibers (bundle A−C and bundle D−F). Each group was bundled together with heat shrink tubing. To equally align the proximal ends of the bundle, each bundle was polished on an Ultra Tec Mfg., Inc. fiber polisher (Santa Ana, CA) with 30-, 9-, 3-, 1-, and 0.3-μm lapping films.

Instrumentation. *Imaging and Analyte Delivery System*. Each fiber bundle was positioned onto a custom-built imaging system with a vacuum-controlled sparging apparatus employed for odor delivery[33] as employed previously.[24] The imaging system employs an inverted Olympus fluorescence microscope incorporating a 75-W Xe excitation source with detection by a 640 × 480 pixel SensiCam high-performance CCD camera (Cooke Corp., Auburn Hills, MI). All testing events employed a 10× (NA 0.30) Zeiss microscope objective.

Analyte Preparation. To deliver the VOCs, a tedlar bag gas dilution odor delivery system was employed as previously described.[13] Three Tedlar bag analytes (air, acetone, toluene) were prepared by adding the proper amount of solvent analyte (none added for "air") with a syringe needle into a flowing diluent air stream (see Supporting Information for sample bag preparation). Solid 1,3-DNB and different types of coffee beans were individually placed in sealed flasks for odor delivery by a vacuum-controlled sparging apparatus. A second blank (air) sample consisted of an empty sealed flask which was purged with air carrier gas. It should be noted that analyte delivery was based on dilution of the saturated odor stream and not by employing calibrated vapor generators. The saturated vapor pressure for 1,3-DNB (as used in this study for quantitative purposes) was 1 part per million (ppm).[34]

Data Collection. The CCD camera captures the fluorescence changes before, during, and after odor exposure to the sensor array by recording image sequences. Each sequence consisted of 45 images with 5 images (e.g., a baseline) captured before analyte delivery, 15 images captured during delivery, and 25 captured postodor delivery. The total duration of each image sequence was 5.44 s with a odor exposure period of 1.81 s. Sixty-five odor observations were recorded for each fiber bundle (bundle A−C and bundle D−F). All testing parameters were identical for each bundle except for the type of neutral density (ND) filter employed to decrease excitation light intensity. For bundle A−C and bundle D−F, 0.25 and 0.6 ND filters were employed, respectively. The excitation and emission filters were 560 (band-pass 40) and 630 (band-pass 20) nm for both bundles. The CCD was binned 2 × 2 and employed 100-ms CCD exposure time. Total air flow was 250 mL/min, and two different delivery systems were used together: a tedlar bag system for acetone and toluene and the sparging system for 1,3-DNB and the three coffee bean types. Responses from a total of 2683 sensors were analyzed, with different numbers of sensors used from each of the six types (see Table 1). The resulting fluorescence signals from identical sensors were combined and averaged to improve detection limits by decreasing the noise in the response. All experiments were performed at room temperature. Odor responses were recorded for all six analytes and the air carrier gas, for a total of 65 observations (Table 2). The highest concentration level for each analyte (and air) was recorded 5 times in order to assess sensor response reproducibility from run to run. Five replicates at highest concentration × seven analytes (5 × 7 = 35 observations) plus five lower concentrations × six analytes (5 × 6 = 30 observations) totals 65 observations.

Table 2. ODOR Concentrations for Observations[a]

air	acetone	toluene	1,3-DNB	three coffee types (% SVP)
(blank)	450	450	0.1	10
	1800	1800	0.2	20
	3600	3600	0.4	40
	5400	5400	0.6	60
	7200	7200	0.8	80
	9000	9000	0.9	90

[a] All exposures are in ppm, except the three coffee types, which were done as percent saturated; i.e., 90% saturation involves 10% air dilution. The highest concentration for each odor was repeated five times.

Image Processing. All 65 odor observations, each consisting of 45 CCD images, were divided into individual files; i.e., each image sequence consisted of 45 individual image files. Image processing was conducted using Labview and IMAQ Vision (National Instruments). A virtual instrument (VI) was programmed to automatically identify beads on the images based around the "IMAQ Circles" sub-VI that is able to fit circles within 2-D images using a least-squares, best-fit criterion.[35] A binary thresholding operation was carried out first on a selected image within the sequence of 45 images for each observation, to generate a binary image required for circle fitting. A single region of interest (ROI) could be specified on the selected image in order to identify the boundaries for a single bead type. After thresholding the image, the VI then fitted circles of variable radius to the image within the ROI. The threshold settings were then optimized for the image sequence in order to obtain the most accurate fitting of bead outlines (least squares) within this region. Once this was achieved, each image within the sequence was processed using the same fitted circle data. For each identified bead, the average gray scale count was calculated for each frame within the sequence. Care was taken to ensure that each bead could be tracked from image to image so that the intensity values could be compared directly between image sequences. In this way it was possible to accurately assess the response from individual beads across the entire collection of image sequences. Figure 1 shows the final fitted circles for each of the six bead types superimposed on the original gray scale images.

By checking the baseline value for a single bead (the average gray scale count before exposure to the analyte) across all of the sequences, we identified some irregularities in the images. On closer inspection, it was clear that a very small amount of

(33) Kauer, J. S.; Shepherd, G. *J. Physiol.* **1977**, *272*, 495−516.
(34) Howard, P. H.; Meylan, W. M. *Handbook of Physical Properties of Organic Chemicals*; Lewis Publishers: New York, 1997.
(35) http://labview.pica.army.mil/the-archives/vi/lv5/beadfinder.zip.

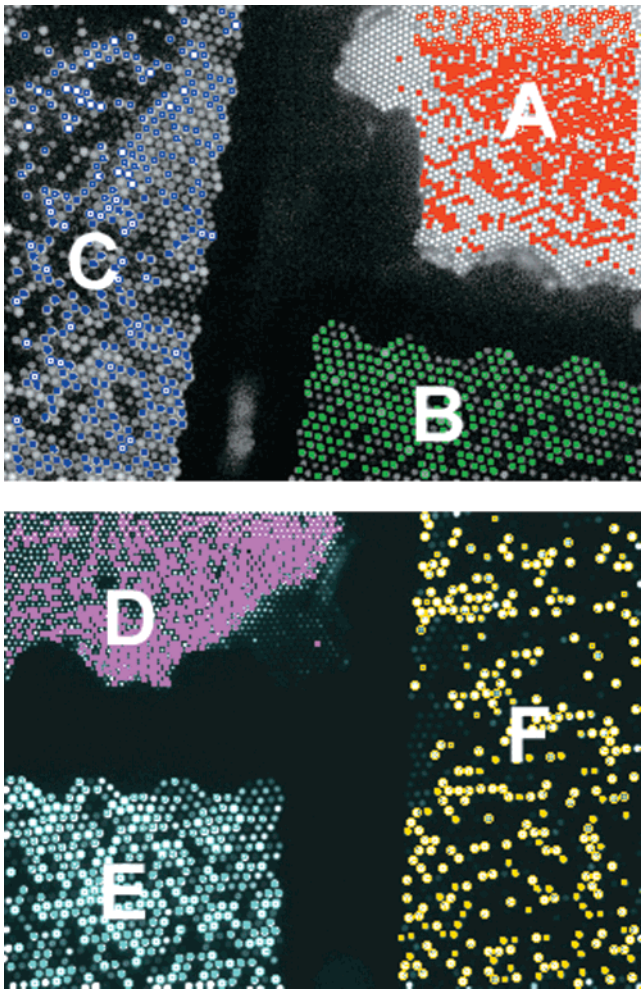

Figure 1. CCD images of each imaging fiber bundle. Bundle A−C (top) and bundle D−F (bottom) showing the fitted ROIs corresponding to each addressable bead sensor. A total of 2683 sensors were analyzed: (A) 814, (B) 286, (C) 301, (D) 692, (E) 294, and (F) 296 beads. The ROIs were automatically generated using Labview and IMAQ Vision software. Each imaging fiber's face is 1 mm^2. Images were acquired with 100-ms exposure time, and excitation/emission filters were 560 (bp 40) and 630 (bp 20) nm, respectively.

movement (1−2 pixels in the *x* or *y* direction) had occurred between the camera and the fiber bundle at specific points during the data collection—an inevitable consequence of the length of time and logistics of operating the equipment. This movement was digitally compensated for by adding software capability to offset the fitted circle data to match the newly relocated bead positions. This arrangement managed to completely remove the discontinuities in the baseline value from test to test. The individual bead response profiles were averaged over all beads of a single type to produce a temporal response profile for each bead type during the 45-image sequence.

RESULTS AND DISCUSSION

In this paper, for the first time, an array of six different Nile Red-stained porous silica beads was employed to monitor and discriminate between both simple and complex odors at various dilutions. Table 1 shows each sensor's composition and the representative population for each of the six sensor types. To simplify the identification of each bead type, we incorporated each microsensor type into the microwells of six different imaging fiber arrays so that each array contained replicates of one sensor type; i.e., each of the six fiber arrays contained replicates of only one of the six bead types. The imaging fibers were then bundled together to create multibead sensor arrays composed of hundreds to thousands of individually addressable micrometer-sized sensor elements (Figure 1). The use of the microsphere sensors permits large quantities of sensors to be deployed in a small area; e.g., each imaging fiber's face is 1 mm^2 and can consist of tens of thousands of individually addressable sensor elements. More than 250 copies of each sensor type are represented (Table 1, Figure 1), and response profiles were recorded before, during, and after odor exposure with a CCD camera for six analytes and also for air carrier gas (Table 2). Sensor response profiles from identical sensor elements for each of the six sensor types were averaged to increase the signal-to-noise (S/N) ratio as shown previously.[13,31] By averaging individual sensor responses, S/N ratios increase and the array's overall dynamic range improves for lower level odors.[13,31] The sensor−analyte response profiles develop immediately upon odor exposure, and the system's rapid response time[13] is progressing toward real-time detection. The sensor−analyte response profiles for each bead were analyzed using Labview and IMAQ Vision processing software (see Experimental Section). Briefly, the CCD sequence for each analyte observation was separated into individual image files and analyzed with respect to fluorescence changes over time for designated sensor elements. The concentration range for 1,3-DNB was 100−900 ppb, and each VOC concentration ranged from 450 to 9000 ppm. The sensors were exposed to six dilution levels for each of the six odors, and the highest relative dilution level for each odor was repeated five times. Including 5 air (blank) responses, 65 odor observations were examined. Although the number of observations is low, the total number of sensors employed is very high; i.e., each sensor's response profile can be considered to be an independent observation. A CCD was employed because it permits many sensor types to be monitored simultaneously and allows uncorrelated noise to be removed by monitoring responses from many individual sensor elements.[13]

Preprocessing Methods. After obtaining each individual sensor element's response over every frame within the series of CCD images, the fluorescence intensity values were averaged over all the identical sensor elements in order to produce a time-dependent response for all six bead types. Figure 2 shows the averaged normalized response profile for each bead type during a single test sequence to each type of odor stimulus. These data show rapid responses with good reversibility, although the bead responses to both 1,3-DNB and hazelnut-flavored coffee odors were noticeably slower in recovering to their original (baseline) values (Figure 2d and e). Four of the six bead types (A, D, E, F) show polarity changes in their response profiles to different odors; i.e., sensor responses show an increase or decrease in fluorescence intensity depending on the analyte, providing valuable additional diversity in the array response as a whole. The other two sensor types did not show polarity changes in their response profiles for the odors tested. Standard preprocessing metrics including fractional, relative, difference, array normalized, and sensor autoscaled (these methods have been detailed widely[3,36])

(36) Pearce, T. C.; Gardner, J. W. *Analyst* **1998**, *123*, 2057−2066.

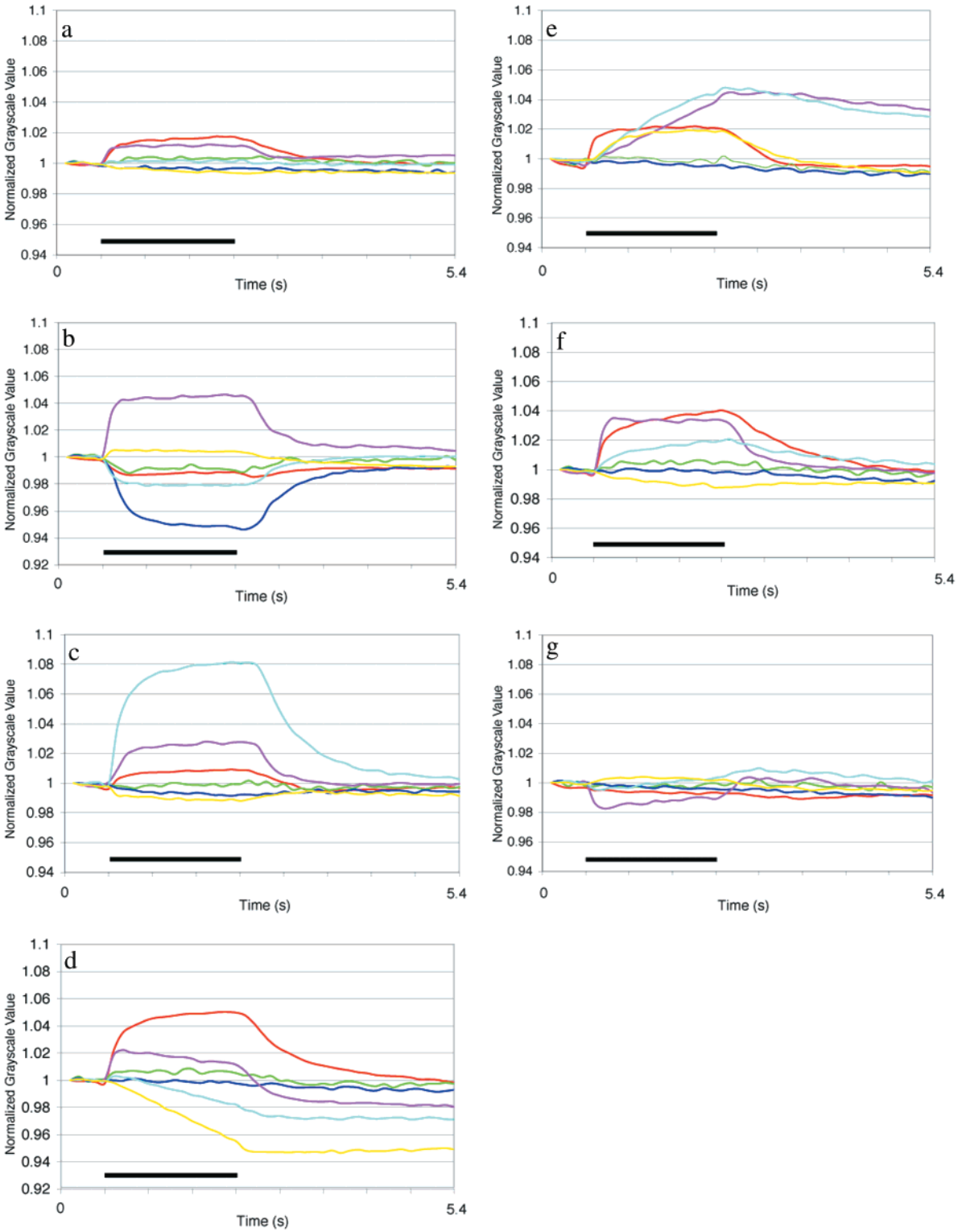

Figure 2. Average normalized time responses for each bead type during a single test sequence to an odor pulse for each of the odor categories: (a) air (control), (b) toluene, (c) acetone, (d) 1,3-DNB, (e) Hazelnut-flavored coffee beans, (f) Columbian coffee beans, and (g) French roast coffee beans. The color coding for each bead type matches that used for Figure 1: A (red); B (green); C (blue); D (magenta); E (aqua); F (yellow). The solid black bar indicates the presence and duration of the 1.81-s odor stimulus.

were used in order to extract a single time-independent parameter for each sensor−analyte combination. Subsequent data processing was conducted for each of these preprocessing metrics in order to reduce bias in the results and permit a quantitative comparison between the metric types.

Exploratory Data Analysis. Radar plots were used to illustrate interclass variation in the bead responses to the highest analyte concentration. Radar plots for the fractional gray scale metric with percent change in response from the initial gray scale baseline values for each of the six bead types to the six odor conditions

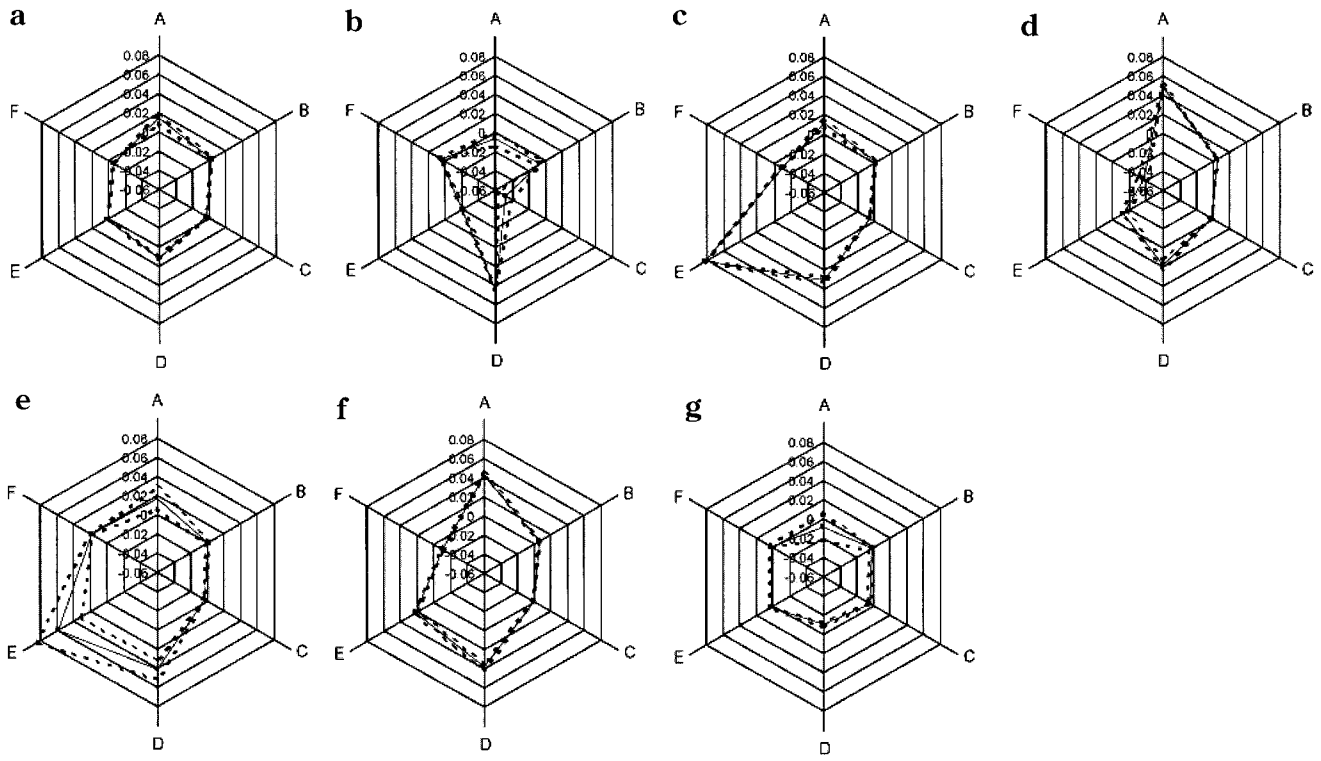

Figure 3. Radar plots showing the difference in the average fractional response to the highest concentrations of each odor class (five repeated runs of each class) for each bead type (A−F) to odors (a−f) as listed in Figure 2. Numbers refer to percent; i.e., 0.06 = 6%. In each case, the dashed lines indicate ±1 SD in the average bead response across the population of sensors analyzed. Positive values indicate an overall increase in gray scale value to the odor while negative values indicate an overall decrease.

and air carrier gas are shown in Figure 3. The fractional values range from −5 (for toluene) to +8% (for acetone). To assess the repeatability of the bead responses, five repeated observations were recorded for each odor class (at maximum concentration). Figure 3 shows the mean of the five highest concentration observations for each class (central solid line) as well as 1 standard deviation (SD) either side of the mean (outer dashed lines), indicating the reproducibility of response for each bead type to each odor class. Interestingly, the radar plots indicate that this reproducibility depends on the odor stimulus. For example, bead type D shows good reproducibility to air, toluene, acetone, 1,3-DNB, Columbian coffee, and French roast coffee beans (Figure 3a−d, f, and g) but less reproducibility to hazelnut-flavored coffee beans (Figure 3e). In general, this kind of observation may be due to some irreversible or temporary poisoning effect between specific odors and the bead type. It is likely that some of the observed response profiles may be less dependent on the concentration of analyte and more dependent on each analyte's relative activity for that sensory material.[37] In this study, odor classifications were not based on analyte concentration because, as shown in Table 2, at least two odors (toluene, acetone) were at the same level for each exposure. We can discriminate between different odor classes even at different concentration levels, so discrimination cannot be based upon different concentration levels alone but must be due to other analyte properties. Every odor class produced significant response profile differences in at least one of the six bead types, which was a good preliminary indication for potential classification between observations and, in general, represents a trivial classification problem at each analyte's highest concentration level. Principal components analysis (PCA) was used as the standard technique to reduce the dimensionality of the data set from *six dimensions to two dimensions* so that data could be visualized directly (see Supporting Information).

Classification Study. For classifying and discriminating between the seven odor conditions, only the averaged bead response profiles (as shown in Figure 2) and data obtained from repeated observations were used. Both multivariate analysis of variance (MANOVA) and discriminant function analysis (DFA) were used for this purpose. MANOVA was applied to the data set in order to assess the effect that odor class had on determining the sensor responses and, therefore, indicated the likely discriminability of the entire data set. Furthermore, the Wilks's λ measure, which indicates the amount of variance not explained by class difference, was used to quantitatively assess the separation of the data for each odor class. Before MANOVA was applied, the underlying assumptions made by the technique, (a) multivariate normality, (b) homogeneity of the covariance matrix, and (c) independence of observations, were tested satisfactorily (see Supporting Information).

The MANOVA procedure was applied to each of the preprocessing types, and the results indicated that, in each case, a very large effect was present between bead response profiles and odor types (Supporting Information). The best performance was achieved by the array normalized fractional gray scale values corresponding to $p < 10^{-3}$ and a Wilks's λ value of 1.08×10^{-7}. This preprocessing metric was therefore selected for odor type

(37) Doleman, B. J.; Severin, E. J.; Lewis, N. S. *Proc. Natl. Acad. Sci. U.S.A.* **1998**, *95*, 5442−5447.

classification using DFA to optimize discrimination performance. The array normalized gray scale values were screened using the Box and Whisker plot and showed no values existed outside of the ±3 SD limit, indicating the absence of deviant data points (Supporting Information).

While the MANOVA results suggest good class separation for all of the preprocessing metrics, canonical DFA analysis was used to construct a set of linear discriminant functions which could be applied as a transformation on the data values to maximally separate the odor categories (Supporting Information). Only the first two out of six discriminant functions were required to adequately classify the seven odor classes (Figure 4a). All five observations for each odor category separate after transformation by the first two discriminant functions. Prescriptive DFA was then performed using the discriminant functions to classify each of the 35 observations into one of 7 odor categories. As shown by the confusion matrix in Table 3, each observation was classified correctly, as indicated by no off-diagonal terms. A classification rate of 100% was achieved for all seven odor observations at their maximum relative concentration levels.

To obtain an indication of the array's detection limit to each of the three simple and three complex odors, the DFA analysis was repeated using the array normalized fractional values, to also include the lower analyte dilutions for the six odor types (Table 2). The challenge was to correctly classify both the maximum concentration observations and the reduced concentration observations into their correct odor categories. The DFA results for the six discriminant functions are shown in Supporting Information. A plot of the transformed preprocessed values is shown in Figure 4b. As in the first classification task, those observations at maximum concentration were shown to effectively separate in DFA space. The results for the diluted observations, however, were not as well separated and, as expected, were harder to discriminate and classify into odor categories. By applying the same discriminant functions to classify each observation, it was possible to achieve 86.2% correct classification over all concentrations. Table 4 shows the confusion matrix for this classification. All the values with "1" (b1, c1, d1, e1, g1) represent the analytes at their lowest concentration, those with "2" (b2, d2, g2) represent the second lowest concentration, followed by "3", etc. Most importantly, Table 4 indicates which of the reduced concentration observations failed to be classified correctly. In most cases, it was the lowest concentration observations that failed to classify correctly, thus indicating the detection limit for this particular array to these analytes. By ignoring the lowest concentration level for each odor, 93.2% classification is achieved, and if the three lowest concentration levels of each odor are ignored, the system classifies all remaining odor observations correctly.

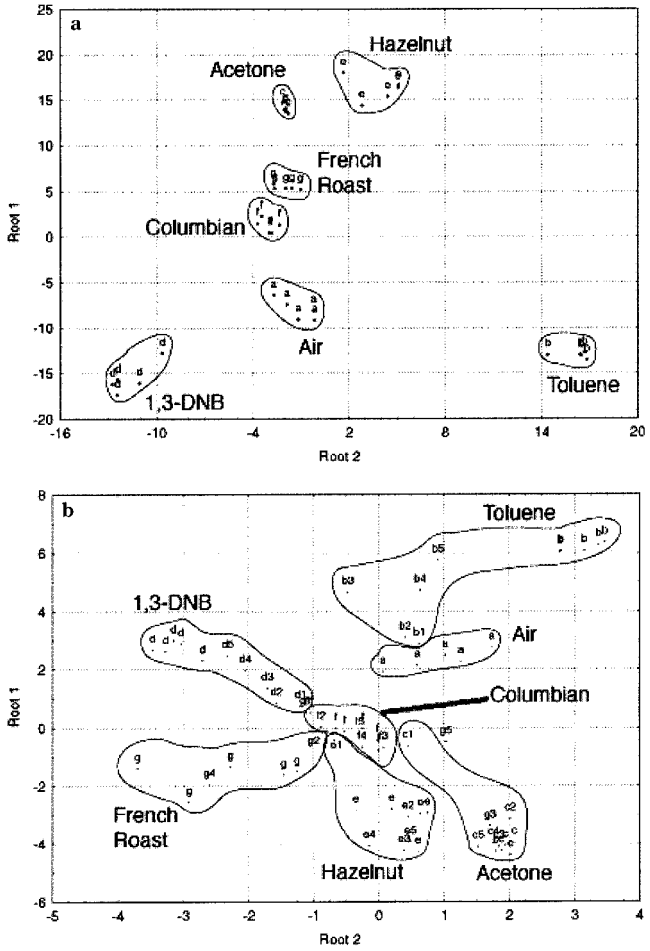

Figure 4. Results of DFA analysis as applied to the array normalized fractional gray scale preprocessed values. (a) First two discriminant functions for maximum odor concentrations of (a−f) as listed in Figure 2. (b) First two discriminant functions for combined maximum and diluted concentrations of the seven odor categories. First letter indicates the odor category, and the second number indicates the concentration level: 1, lowest concentration; 2, second lowest concentration; etc.; no number, highest concentration.

CONCLUSIONS

A fiber optic, bead sensor array that can accurately discriminate between six analytes at various dilutions has been described.

Table 3. Confusion Matrix Produced by Applying Prescriptive DFA to the Array Normalized Fractional Preprocessed Gray Scale Values Obtained from 35 Observations at Maximum Concentration[a]

	predicted class						
actual class	air	toluene	acetone	DNB	hazelnut-flavored coffee	Columbian coffee	French roast coffee
air	**5**	0	0	0	0	0	0
toluene	0	**5**	0	0	0	0	0
acetone	0	0	**5**	0	0	0	0
DNB	0	0	0	**5**	0	0	0
hazelnut-flavored coffee	0	0	0	0	**5**	0	0
Columbian coffee	0	0	0	0	0	**5**	0
French roast coffee	0	0	0	0	0	0	**5**

[a] The average classification rate is 100%.

Table 4. Confusion Matrix Produced by Applying Prescriptive DFA to the Array Normalized Fractional Preprocessed Gray Scale Values Obtained from 35 Samples at Maximum Concentrations and 30 Samples at Diluted Concentration[a]

	predicted class						
actual class	air (a)	toluene (b)	acetone (c)	DNB (d)	hazelnut-flavored coffee (e)	Columbian coffee (f)	French roast coffee (g)
air (a)	**5**	0	0	0	0	0	0
toluene (b)	**2 (b1, b2)**	**8**	0	0	0	0	0
acetone (c)	0	0	**9**	0	0	**1 (c1)**	0
DNB (d)	0	0	0	**8**	0	**2 (d1, d2)**	0
hazelnut-flavored coffee (e)	0	0	0	0	**9**	**1 (e1)**	0
Columbian coffee (f)	0	0	0	0	0	**10**	0
French roast coffee (g)	0	0	**1 (g3)**	0	0	**2 (g1, g2)**	**7**

[a] Average classification rate 86.2%. Samples with "l" refer to lowest concentration.

Discrimination of two VOCs, one NAC, and three coffee bean odors with 100% correct classification was achieved at the highest relative concentration levels (within the data set), and the system was also capable of achieving discrimination at various dilutions. The six sensor materials employed in our study were not preselected in any fashion as being particularly good transducers for any of the six odor types, including three types of coffee beans, and air. Yet the sensors were able to fully discriminate all analytes without any sensor−analyte optimizations. This study complements our previous bead-based vapor detection efforts which mainly focused on two-class problems for detecting the presence/absence of specific vapor targets.[14−16] In terms of comparison with other electronic noses, we clearly demonstrate that bead-based sensors can discriminate complex odors, which brings our technology in line with other sensor technologies and proves that it is a viable approach for complex odor discrimination. With the given speed of the fluorescence-based system (faster than other documented nose chemosensors), there is the chance that near-continuous real-time monitoring could take place for industrial process control, as well as food monitoring or smoke detection. The sensors show good reversibility, speed, and diversity to a broad range of organic compounds, making them ideal for both odor classification and individual component concentration prediction tasks. The reproducibility of sensor types has been quantified, as have the relative detection limits to the battery of compounds tested. The properties of this system are also ideal for modeling the olfactory system[32] and can be used to improve on any practical applications of this array platform, that is, the ability to produce multiple sensor arrays with transferable computational classifiers.[16]

ACKNOWLEDGMENT

The Tufts work is supported by the Defense Advanced Research Projects Agency and the Office of Naval Research and the Leicester work is funded by the Royal Society, London.

SUPPORTING INFORMATION AVAILABLE

Details of the statistical techniques, tables of PCA, MANOVA, and DFA analyses, and figures of PCA and Box and Whisker plots for the odor categories. This material is available free of charge via the Internet at http://pubs.acs.org.

Received for review September 22, 2000. Accepted March 23, 2001.

AC001137A